Voltage imaging with ANNINE dyes and two-photon microscopy of Purkinje dendrites in awake mice

Technologies Advancing Neuroscience

Voltage imaging with ANNINE dyes and two-photon microscopy of Purkinje dendrites in awake mice

***Christopher J. Roome*[1*], *Bernd Kuhn*[1*]**

[1]OIST Graduate University, 1919-1 Tancha, Onna-son, Okinawa, Japan

[*]chris.roome@oist.jp, bkuhn@oist.jp

Research Highlights

- ANNINE dyes are purely electrochromic voltage sensitive dyes with linear, nanosecond responses
- Red spectral edge excitation increases voltage sensitivity and reduces phototoxicity and bleaching
- Dendritic voltage signals can be studied in awake animals using two-photon imaging
- Voltage and calcium imaging, pharmacology, or electrical recordings can be combined
- Subthreshold dendritic voltage signals reveal a 5µm basic unit of dendritic computation

Abstract

Voltage imaging is the next generation of functional imaging in neuroscience. It promises to resolve neuronal activity 10 to 100-times faster than calcium imaging and to report not only supra but also subthreshold activity on a single cell or even subcellular level. Lately, several different voltage sensors and imaging techniques were published which can achieve this. Here, we focus on a technique based on the synthetic pure electrochromic voltage-sensitive dyes ANNINE-6 and ANNINE-6plus and the excitation of this dye at the red spectral edge of absorption to maximize voltage sensitivity and minimize phototoxicity and bleaching. Importantly, voltage imaging with ANNINE dyes can be done with one and two-photon excitation. Two-photon microscopy allows in vivo, depth resolved imaging and line-scan recordings with sub-millisecond temporal resolution. Interestingly for many future applications, the spectral characteristics of ANNINE dyes allows simultaneous imaging with green indicators, like the genetically encoded calcium indicator GCaMP6. We used this method to study supra and subthreshold dendritic voltage changes in Purkinje neurons of awake mice. Simultaneously, we imaged dendritic calcium and recorded electrical activity from the soma or locally applied drugs to show the full potential of the technique to study dendritic integration in awake animals.

Introduction

Observing the brain at work on a cellular level is the dream of many neuroscientists. We would love to see how neuronal activity triggered in the retina of our eye travels to the brain, how this activity is transmitted from neuron to neuron, how this information of the outside world is processed and integrated in the persistent neuronal network activity, and thereby update our brain-internal model of the outside world and ourselves. This dream has already come true to some extent: there are several methods available to image neuronal calcium activity of thousands of neurons and their processes in awake animals (Chen et al 2013) with indicators which are based on a single, circularly permutated green fluorescent protein fused to a calcium binding domain (Nakai et al 2001). However, to image the electrical activity in the mammalian brain on a cellular or sub-cellular level is still a challenge. Electrical signals in the brain typically last only one millisecond and therefore imaging must be even faster to capture such signals.

Voltage imaging was one of the first functional imaging methods developed, and the earliest reports go back 50 years (Cohen et al 1974, Tasaki et al 1968). Using optimized synthetic voltage-sensitive dyes and fast cameras, voltage was successfully imaged, for example, from neuronal networks in invertebrates (Grinvald et al 1977, Senseman & Salzberg 1980), brain slices (Iijima et al 1996), brain modules in vivo (Grinvald & Hildesheim 2004, Grinvald et al 1986), and single neurons and their compartments in brain

slices (Antic et al 1999, Antic & Zecevic 1995). However, voltage imaging in mammalian tissue in vivo with single cell resolution or subcellular resolution failed because no method has been available for labeling specific subgroups of neurons with synthetic dyes. If synthetic voltage-sensitive dyes are injected into tissue or applied to the brain surface, they unspecifically label all cell surfaces in tissue, with axons, dendrites, and astrocyte processes being the main plasma membrane contributors. Due to the dense packing of these processes, the single structures cannot be optically resolved and only average membrane potential changes can be measured.

Already 20 years ago, also genetically encoded voltage indicators were developed (Knöpfel 2012). Their key advantage is that they can be targeted to specific cell types. Over the last few years their sensitivity and temporal resolution have reached a very promising performance level. However, millisecond-resolution single-cell-resolved voltage imaging with genetically encoded indicators in scattering tissue is still not possible.

Recently, a promising hybrid approach was published, expressing a genetically encoded voltage sensor with a domain to bind washed-in synthetic dye to enhance the fluorescence intensity (Abdelfattah et al 2019). It allows to image populations of neurons in different types of tissue. This hybrid indicator system can so far not be used with two-photon microscopy, but it has a great potential to do so in the near future.

Here, we first summarize our voltage imaging approach which is based on the synthetic voltage-sensitive dyes ANNINE-6 and ANNINE-6plus. An in-depth primer of the method (Kuhn & Roome 2019) and detailed protocols (Roome & Kuhn 2019) were published previously. In the second part, we give an example of voltage imaging from dendrites of Purkinje neurons in awake mice (Roome & Kuhn 2018).

Voltage sensing mechanism of ANNINE dyes

About 20 years ago, we developed a novel family of synthetic voltage-sensitive dyes, in chemical terms anellated hemicyanines, short ANNINEs (Hübener et al 2003, Kuhn & Fromherz 2003). The ANNINE dyes, here represented by ANNINE-6 and ANNINE-6plus (Fromherz et al 2008) with a 6-ring chromophore (Fig. 1a), are similar in most respects to other voltage-sensitive dyes like di-4-ANEPPS (Fig. 1a) (Fluhler et al 1985) or RH-160 (Grinvald et al 1982). They have a hydrophobic tail group and a hydrophilic head group. The headgroup of ANNINE-6 has a positive and a negative charge, while ANNINE-6plus has two positive charges which makes it less hydrophobic. The amphiphilic design allows these dyes to bind to lipid membranes (Fig. 1b). Their chromophore is formed by C and N atoms connected by conjugated single-double bonds. As a result of this bonding type the electrons involved in the π-bond are delocalized and their

orbitals define the chromophore. These electrons are bound weakly and therefore the energy of a single photon in the visible wavelength range, typically blue, is enough to excited one of the outermost electrons from the ground state to an excited state. Importantly, the chromophore is elongated and asymmetric; aniline forms one end, pyridinium the other. As a result of this asymmetry the center of charge of the delocalized electrons is shifted towards aniline due to its higher electronegativity than pyridinium (Fig. 1c, center). However, if one of the delocalized electrons gets excited by the absorption of a photon it is pulled toward pyridinium and pushed away from aniline (Fig. 1c, center). So, a charge moves along the elongated axis of the molecule.

The special feature of ANNINE dyes is that the chromophore is fully anellated. This makes the chemical synthesis difficult, but the advantage is that the anellation prohibits conformational changes within the chromophore due to rotation around single bonds or flipping at double bonds. ANNNE chromophores are rigid. Conformational changes as rotations and flipping are associated with triplet state generation, bleaching, and phototoxicity (Ephardt & Fromherz 1993, Röcker et al 1996). Conformational changes might be also associated with movement of the dye at the membrane-water interface, resulting in a fluorescence change that interferes with fluorescence changes due to the voltage sensing mechanism.

The design of the voltage-sensitive dye molecules with two carbohydrate chains and an elongated chromophore ensures that the molecule axis is roughly aligned with the membrane normal. If the molecule axis is aligned to the membrane normal and there is an electric field over the membrane, then the charge movement within the molecule will be modulated by the external electric field over the membrane (Fig 1c, left and right). For example, if the delocalized electron is shifted against the external electric field, less energy is needed compared to no external electric field because the field pulls the electron (Fig. 1c left). Therefore, the absorption spectrum shifts to lower energy, that is to longer wavelength. During the emission process, the electron moves with the electric field and therefore loses energy. Hence, also the emission spectrum will be shifted to lower energy. If the external electric field turns, as during an action potential, the excitation and emission spectrum will be shifted to higher energy, that is shorter wavelength (Fig. 1c right). If there are no other mechanisms of fluorescence change involved, the energy shift of both, the excitation and emission spectrum, should be the same. Importantly, ANNINE dyes are so far the only voltage-sensitive dyes which show this pure electrochromic effect where excitation and emission spectrum are shifted by the same energy (Kuhn & Fromherz 2003). Additionally, ANNINE-6 exhibits the largest so far measured charge shift in any voltage-sensitive dye. The charge shifts by 0.81 nm within the chromophore (Kuhn & Fromherz 2003).

For voltage-sensitive dyes of this type only the spectra are shifted but the amplitude of the spectrum remains unchanged. Unfortunately, the spectral shift is only very small (a few nanometer) as the external electric field over the membrane and its changes are small in comparison with the electric fields within the dye molecule. This contrasts with the widely used calcium indicators for which the amplitude is changing upon binding of calcium ions while the spectral shape remains almost unchanged.

One advantage of ANNINE dyes is that the effect is purely based on the interaction of the charge in the molecule and the electric field. As a result, the responses are linear and not influenced by diffusion processes, conformational changes, or binding processes as for calcium indicators. Also, ANNINE dyes do not move within the membrane and the chromophore conformation cannot change due to the anellation. Other voltage-sensitive dyes move and can change their confirmation which influences their fluorescence. Also, as the voltage-sensing mechanism is purely based on the interaction of a charge with an electric field, the so-called molecular Stark effect (Kuhn & Fromherz 2003, Stark 1914), voltage imaging with ANNINE dyes is independent of the membrane composition which makes the ANNINE dyes applicable in very different tissue. Another advantage of using a pure molecular Stark-shift probe is that the responses are almost instantaneous. For example, ANNINE-6 was used to resolve membrane voltage changes on a nanosecond time scale (Frey et al 2006).

Voltage imaging with ANNINE dyes

Detectors, like camera sensors or photomultiplier tubes detect changes in fluorescence intensity. To convert the spectral shift of the voltage-sensitive dyes into a measurable intensity change, spectral band pass filters for excitation and emission are used. Here, as an example, we show the excitation spectrum of ANNINE-6 labeling the outer leaflet of the plasma membrane at resting potential (Fig. 2a, black spectrum). If the voltage changes by 100 mV, the excitation spectrum shifts by about 3 nm (Fig. 2a, red spectrum). The difference between two spectra is called the fluorescence change ΔF (Fig. 2b). The fluorescence change normalized with the fluorescence spectrum results in the relative fluorescence change (Fig. 2c). Simplified, there are two basic strategies to optimize the voltage signal, differing in the excitation light source.

If a white light source with the overall intensity distributed over a wide spectral range, such as a Xe-arc or halogen lamp, and a band pass filter is used for excitation, it is best to choose the excitation filter so that at the steepest slope of the spectrum is excited (Fig. 2a-c, blue arrows). Whenever the spectrum is shifted, this will result in the largest signal, that is the largest fluorescence change (in this case, a decrease in intensity). However, the sensitivity is relatively low and, therefore, many photons are needed to detect a signal. A

signal can only be detected if it overcomes the noise intrinsic to any optical measurement. Importantly, the number of generated photons is proportional to phototoxicity caused by the excited dye. This is typically not a problem for bulk loaded tissue but hampers recordings from fine structures as dendrites or axons.

The second strategy is to use a light source with almost unlimited intensity, i.e. lasers, for excitation and to optimize the relative fluorescence change (Kuhn et al 2004). As the relative fluorescence change is normalized to the number of detected photons, it is proportional to information about the voltage change gained per detected photon. In this case it is best to excite at the spectral edge (Fig. 2a-c, black arrow) where the relative fluorescence change is largest. However, the excitation spectrum corresponding to the excitation probability is here very low (only a few % of the maximum) and, therefore, a white light source, e.g. Xe-arc or halogen lamp, for excitation has insufficient intensity to generate a fluorescence intensity which overcomes the photon shot-noise. This problem can be overcome by using lasers to excite. So, a very high excitation intensity is required to achieve a useful fluorescence intensity, but at the spectral edge the fluorescence change will be large as the relative fluorescence change is large. Important to note is that light by itself is not harmful to tissue if it is not absorbed. Using high excitation intensity at the red spectral edge is thus within a range that does not disturb or damage the tissue. With excitation at the red spectral edge of the absorption spectrum, ANNINE-6 achieves a sensitivity of about 50% per 100 mV voltage change. Additionally, bleaching or phototoxic effects are neglectable due to the low number of excited dye molecules necessary to achieve a large optical signal for a voltage change. Additionally and for all fluorescent molecules, it can be assumed that excitation at the red spectral edge of absorption is less harmful as the smallest amount of energy is absorbed to generate an electronically excited state (Kuhn & Roome 2019).

Summarizing, the strategy for optimizing voltage imaging depends on the light source available. White light sources such as Xe-arc lamps or halogen lamps are typically very stable light sources but only achieve a limited relative fluorescence change. Alternatively, with lasers, high sensitivities can be achieved, but some lasers tend to be less stable than white light sources and, for wide field excitation the speckle pattern, resulting from the coherence of the laser light, hampers their applicability. For wide field imaging with bright signals, both strategies work. However, for voltage imaging of fine structures, where bleaching and phototoxicity affect the experiments, excitation with lasers at the red spectral edge of absorption becomes crucial. Bright LED light sources, if available with a spectrum in the range between the steepest slope and the spectral edge of the excitation spectrum, might bridge these two strategies

Labeling with synthetic voltage-sensitive dyes can be achieved by bath application to cell cultures or injection into tissue in vivo. If the dye is externally applied, it will bind to the outer leaflet of the lipid

bilayer membrane. A depolarization of the membrane results in a decrease of the fluorescence intensity. The advantage of this approach is that the labeling is easy to achieve. The disadvantage is that all membrane surfaces are labeled, including glia, so that it is typically not possible to extract signals from a single neuron. Using this approach, ANNINE dyes can be used to measure, for example, voltage changes of single neurons in cell cultures (Pages et al 2011) or average membrane voltage changes and oscillations in vivo (Kuhn et al 2008).

If the voltage-sensitive dye is intracellularly applied the dye will label the inner leaflet of the lipid membrane. As the orientation of the dye in respect to the electric field over the membrane is reversed in comparison to the extracellular application, the signal turns: The intensity increases with a depolarization of the cell. The filling of single cells is tedious but allows to image the voltage from dendrites and axons in vitro and in vivo (Antic et al 1999, Antic & Zecevic 1995, Roome & Kuhn 2018).

In general, voltage-sensitive dyes can flip from one leaflet of the lipid bilayer to the other until an equilibrium is reached based on statistics and the dye's charge. If the dye will be equally distributed on both sides, the voltage signal disappears. If the dye has a net charge the signal might even turn. Interestingly, ANNINE dyes barely flip and show a similar sensitivity even after 2 weeks in vivo when intracellularly applied (Roome & Kuhn 2018). Also when extracellularly applied to HEK293 or primary cell cultures ANNINE dyes barely flip or internalize allowing extended imaging sessions (Pages et al 2011).

Voltage imaging is typically performed with one-photon excitation and cameras detection. In this case, huge numbers of photons can be detected reducing the relative photon noise (photon noise divided by the average number of detected photons). However, in scattering tissue as in the mammalian brain the spatial resolution is limited. Two-photon microscopy can partly overcome the scattering problem (Helmchen & Denk 2005). Additionally, two-photon microscopy allows optical sectioning. Due to the sectioning, the number of excited dye molecules and detected photons is typically orders of magnitudes lower than with wide-field one-photon excitation and camera imaging. Therefore, the relative photon noise is much higher. ANNINE dyes can be easily excited at the red spectral edge of absorption with confocal microscopy (Kuhn et al 2004, Pages et al 2011) and with two-photon microscopy, where the sensitivity increases (Fig. 2d-h) (Kuhn et al 2008, Kuhn et al 2004, Roome & Kuhn 2018).

Finally, ANNINE-6 dyes can be easily combined with green calcium indicators, like GCaMP, because of their spectral properties. This compatibility will allow a wide range of novel experiments.

The applicability of ANNINE dyes in neuroscience was previously demonstrated in neuronal cell cultures (Pages et al 2011), in bulk loaded tissue in anesthetized and awake animals (Kuhn et al 2008), and, recently, to image voltage in the dendrites of single Purkinje neurons in awake mice (Roome & Kuhn 2018).

To give an example of the full potential of the technique, we focus in the following paragraphs on the Purkinje dendrite experiments (Roome & Kuhn 2018). At first, we argue for the importance of studying dendritic integration under fully physiological conditions and the difficulties faced to do so. Then, we explain the experimental design to overcome these difficulties and summarize our findings.

Why study dendritic integration with voltage imaging in awake animals?

Dendritic information processing is fundamental to how neurons work, and consequently, to how we perceive and interact with the world around us. The elaborate geometries of neuronal dendrites, their non-linear electrical properties, and the distribution and strength of their varied synaptic inputs, enables neurons to perform complex computations (Häusser et al 2000, Stuart & Spruston 2015). The computations underlying how we respond to sensory input and learn to make controlled movements for example, is thought to occur through rapid spatio-temporal decoding of signals generated at dendritic synapses of individual neurons, at the scale of microns and milliseconds (London & Häusser 2005, Segev & London 2000).

Over 60 years of experimental and theoretical studies devoted to understanding dendritic function have provided great insight into the complex processing that dendrites can perform (Stuart et al 2016). However, due to technological limitations, most experiments have been performed in brain slices and therefore lack the synaptic inputs that occur in awake behaving animals. These key components are essential for understanding dendritic signal processing in living animals.

Dendritic signal processing in the intact brain remains elusive, especially when investigating how dendritic input influences somatic activity (neuronal output), also known as ‘dendritic integration’. This is predominantly due to the technical limitations of recording from soma and dendrites simultaneously in awake animals.

A well-known example of dendritic integration involves action potential back-propagation, whereby a somatic action potential signal propagates backwards into the dendrites (Waters et al 2003) (in addition to forwards along the axon). In doing so, it is thought to communicate a message of successful somatic action potential generation to active dendritic synapses, and thereby modulate synaptic plasticity through local dendritic calcium influx. This form of dendritic processing occurs in several neuron types, including

neocortical pyramidal neurons, and has been well-studied in brain slices (Stuart & Sakmann 1994). Back-propagating action potentials are thought a key mechanism underlying how we learn and build memories (Svoboda et al 1999). Their function in the intact brain, however, is highly controversial, if or how back-propagating action potentials contribute during learning and memory remains unknown.

Another important example of dendritic integration thought to occur in cerebellar Purkinje neurons is coincidence detection, whereby temporally coincident synaptic input from two distinct excitatory synaptic inputs, parallel fibers and climbing fibers, is thought to trigger a neuronal signal that modifies the strength of parallel fiber input to Purkinje neuron synapses, through synaptic plasticity (Ito 2000, Wang et al 2000).

Electrical recording in vivo (Margrie et al 2002), and somatic whole-cell recording in particular (Petersen 2017), has provided many insights into how neurons behave in their natural environment. However, electrical recording from neuronal dendrites in vivo is challenging, and is often limited to anaesthetized animals (Smith et al 2013) or restricted to single dendritic processes with limited spatial resolution across the neuron (Moore et al 2017). Importantly, although generally considered the current state-of-the-art, these techniques do not allow voltage and calcium recording from the finest spiny dendritic processes, that receive the majority of synaptic inputs.

On the other hand, optical functional imaging techniques in awake animals combining two-photon microscopy (Denk et al 1990), chronic cranial windows (Holtmaat et al 2009) and genetically encoded indicators (Chen et al 2013) provide high spatio-temporal resolution from spiny dendrites (Yang & Yuste 2017). However, these techniques typically only use calcium indicators, reporting supra-threshold dendritic signals at a temporal resolution limited by second messenger and indicator dynamics.

Thus, despite its importance, recording rapid (~ 1ms) signals from fine (< 1µm) dendritic processes in awake animals is not possible through conventional approaches. Novel optical recording techniques designed to overcome these limitations have been eagerly anticipated. Specifically, high resolution spatio-temporal mapping of dendritic signaling using simultaneous voltage and calcium imaging is essential for investigating dendritic integration in awake animals.

Simultaneous voltage and calcium imaging from dendrites and electrical somatic recording from Purkinje neurons in awake mice

By combining simultaneous sub-millisecond voltage and calcium two-photon imaging from spiny dendrites with somatic electrical recording, we investigated dendritic processing of spontaneously active cerebellar Purkinje neurons (PNs) in awake resting mice. These multidimensional dendritic-somatic recordings are

the first to be conducted in an awake animal, serving as an introduction to the much-anticipated field of voltage imaging from neuronal dendrites in behaving animals.

Several experimental challenges had to be overcome to do the experiments (Fig. 3).

Chronic cranial windows have been instrumental in advancing in vivo optical imaging studies, permitting long-term high-resolution imaging in various brain regions in awake animals, however it does not allow to access the brain. Using a simple modification to the chronic cranial window technique we incorporated a sterile silicone access port into the window (Fig. 3a) that permits long-term repeated physical and optical access to the brain (Fig. 3b) (Roome & Kuhn 2014).

Filling single neurons with ANNINE-6plus turned out to be a real challenge. However, ANNINE-6plus dissolves well in ethanol (Fig. 3c) and we used this ANNINE-6plus/ethanol solution to labelled individual neurons in vivo under a two-photon microscope (Fig. 3d) by electroporation (Fig. 3e-h). After some practice, the electroporation procedure is a reliable way to fill Purkinje neurons in vivo (Fig. 3i-k) and also other neurons such as cortical pyramidal neurons (Fig. 3l).

The chronic cranial window with access port also allowed us to perform simultaneous electrophysiology or pharmacological manipulations and optical imaging on awake mice over several weeks (Roome & Kuhn 2018). Since animals recover quickly from surgery and can be used repetitively for many weeks (until bone regrowth obscures the window), behavioral training may be implemented. Perhaps equally important, the total number of animals used in research is significantly reduced, while the information gained from a single animal is dramatically increased.

We double-labelled single cerebellar Purkinje neurons with ANNINE-6plus and GCaMP6f for simultaneous dendritic voltage and calcium imaging. To reduce phototoxicity and increase signal amplitude, we excited at the red spectral edge of absorption (1020nm). Using line scans (position indicated in Fig. 3k) at a temporal resolution of 2 kHz we simultaneously recorded voltage and calcium signals from the PN spiny dendrites (Fig. 4a,b). Extracellular electrophysiology was performed at the labelled PN soma to record somatic activity (Fig. 4c). Pharmacological manipulations were also used to identify the voltage and calcium dendritic signals that we recorded and importantly, these dendritic recordings could be repeated for up to two weeks in an awake mouse (Roome & Kuhn 2018, Roome & Kuhn 2019).

Our results confirmed many findings that were described previously only in brain slices, including highly attenuated back-propagating action potentials in the PN dendrites (Roome & Kuhn 2018). Dendritic voltage imaging revealed spatio-temporal dendritic signaling patterns in PNs that was far more complex, dynamic, and fine scaled than previously anticipated, and surprisingly, even in resting animals. We observed discrete

1−2 ms suprathreshold voltage spikelets that invaded the distal spiny dendrites during dendritic complex spike events (Fig. 4d). These spikelets and their calcium correlates are highly variable in number, timing and most striking, in their spatial variability, such that the number of calcium spikelets generated by a single climbing fiber input varied across different dendritic regions to produce fully spatially and temporally graded calcium signals evoked by the formally assumed monolithic ('all-or-none') complex spike event (Fig. 4d).

Dendritic voltage imaging also detected rapid subthreshold voltage signals evoked by parallel fiber synaptic input for the first time in vivo (Fig. 5a, also visible in Fig. 4a). These events, we refer to as 'hotspots', were localized to fine dendritic processes and had no corresponding calcium signal. Hotspots were partially blocked by AMPA/kainate antagonist (CNQX) and by Na^+ channel antagonist (lidocaine) and showed regimes of linear and nonlinear relationship with the somatic simple spike firing rate (Fig. 5c-d) (Roome & Kuhn 2018). It was surprising to find that hotspot synaptic EPSPs were remarkably fast (5–10 ms) and localized to short (~5μm) dendritic segments, with a shorter apparent length constant than had been predicted from computational modelling techniques (De Schutter & Bower 1994b, Roth & Häusser 2001). It is worth noting however that the spatial extent of these signals agrees well with clustered co-activated synaptic input observed in layer 2/3 pyramidal neurons in the cortex (Scholl et al 2017, Wilson et al 2016), and supports theories for spatio-temporally clustered synaptic input and fine-scale (5-10 micrometer) units of dendritic computation in vivo (Larkum & Nevian 2008, Wilms & Häusser 2015, Yasuda & Murakoshi 2011). It is likely that the EPSP length constant is modulated by intrinsic dendritic mechanisms (i.e. active and passive channels) and/or coincident synaptic mechanisms, such as through feedforward inhibition via molecular interneurons (De Schutter 1998, De Schutter & Bower 1994a, Mittmann et al 2005).

In addition to the well-known climbing fiber evoked dendritic calcium spikes, we also detected rare non-climbing fiber evoked dendritic spikes that occurred following a sharp increase in hotspot activity in the spiny dendrites (Fig. 5a and e). Unlike climbing fiber evoked dendritic spikes, dendritic spike events generated a smaller localized elevation in dendritic calcium and with no associated somatic signal. Parallel fiber evoked dendritic spikes had not previously been observed in vivo. PF evoked dendritic spike events frequently follow climbing fiber evoked dendritic complex spike events, and thus contribute to the overall dendritic calcium signal. Our findings indicate that a strong increase in parallel fiber input evoked by sensory stimulation, for example, may function to enhance dendritic calcium influx if a coincident climbing fiber-evoked event occurs. This form of dendritic coincidence detection of parallel fiber and climbing fiber input is known to induce long-term depression (LTD) at PF-PN synapses (in brain slices) (Wang et al 2000) and is thought a key mechanism underlying learning for the control of movements by the cerebellum.

Acknowledgement

The authors thank the Okinawa Institute of Science and Technology Graduate University for internal funding.

Author Contributions

C.J.R. and B.K. wrote the manuscript.

Conflict of Interest Statement

The authors have no conflict of interest.

References

Abdelfattah AS, Kawashima T, Singh A, Novak O, Liu H, et al. 2019. Bright and photostable chemigenetic indicators for extended in vivo voltage imaging. *Science* 365: 699-704

Antic S, Major G, Zecevic D. 1999. Fast optical recordings of membrane potential changes from dendrites of pyramidal neurons. *J Neurophysiol* 82: 1615-21

Antic S, Zecevic D. 1995. Optical signals from neurons with internally applied voltage-sensitive dyes. *J Neurosci* 15: 1392-405

Chen TW, Wardill TJ, Sun Y, Pulver SR, Renninger SL, et al. 2013. Ultrasensitive fluorescent proteins for imaging neuronal activity. *Nature* 499: 295-300

Cohen LB, Salzberg BM, Davila HV, Ross WN, Landowne D, et al. 1974. Changes in axon fluorescence during activity - Molecular probes of membrane potential. *J Membrane Biol* 19: 1-36

De Schutter E. 1998. Dendritic voltage and calcium-gated channels amplify the variability of postsynaptic responses in a Purkinje cell model. *Journal of neurophysiology* 80: 504-19

De Schutter E, Bower JM. 1994a. An active membrane model of the cerebellar Purkinje cell II. Simulation of synaptic responses. *Journal of neurophysiology* 71: 401-19

De Schutter E, Bower JM. 1994b. Simulated responses of cerebellar Purkinje cells are independent of the dendritic location of granule cell synaptic inputs. *Proceedings of the National Academy of Sciences of the United States of America* 91: 4736-40

Denk W, Strickler JH, Webb WW. 1990. Two-photon laser scanning fluorescence microscopy. *Science* 248: 73-6

Ephardt H, Fromherz P. 1993. Fluorescence of amphiphilic hemicyanine dyes without free double-bonds. *J Phys Chem* 97: 4540-47

Fluhler E, Burnham VG, Loew LM. 1985. Spectra, membrane-binding, and potentiometric responses of new charge shift probes. *Biochem* 24: 5749-55

Frey W, White JA, Price RO, Blackmore PF, Joshi RP, et al. 2006. Plasma membrane voltage changes during nanosecond pulsed electric field exposure. *Biophys J* 90: 3608-15

Fromherz P, Hübener G, Kuhn B, Hinner MJ. 2008. ANNINE-6plus, a voltage-sensitive dye with good solubility, strong membrane binding and high sensitivity. *Eur Biophys J Biophy* 37: 509-14

Grinvald A, Hildesheim R. 2004. VSDI: A new era in functional imaging of cortical dynamics. *Nat Rev Neurosci* 5: 874-85

Grinvald A, Hildesheim R, Farber IC, Anglister L. 1982. Improved fluorescent probes for the measurement of rapid changes in membrane potential. *Biophys J* 39: 301-08

Grinvald A, Lieke E, Frostig RD, Gilbert CD, Wiesel TN. 1986. Functional architecture of cortex revealed by optical imaging of intrinsic signals. *Nature* 324: 361-4

Grinvald A, Salzberg BM, Cohen LB. 1977. Simultaneous recording from several neurones in an invertebrate central nervous system. *Nature* 268: 140-2

Häusser M, Spruston N, Stuart GJ. 2000. Diversity and dynamics of dendritic signaling. *Science* 290: 739-44

Helmchen F, Denk W. 2005. Deep tissue two-photon microscopy. *Nat Methods* 2: 932-40

Holtmaat A, Bonhoeffer T, Chow DK, Chuckowree J, De Paola V, et al. 2009. Long-term, high-resolution imaging in the mouse neocortex through a chronic cranial window. *Nat Protoc* 4: 1128-44

Hübener G, Lambacher A, Fromherz P. 2003. Anellated hemicyanine dyes with large symmetrical solvatochromism of absorption and fluorescence. *J Phys Chem B* 107: 7896-902

Iijima T, Witter MP, Ichikawa M, Tominaga T, Kajiwara R, Matsumoto G. 1996. Entorhinal-hippocampal interactions revealed by real-time imaging. *Science* 272: 1176-9

Ito M. 2000. Mechanisms of motor learning in the cerebellum. *Brain Res* 886: 237-45

Knöpfel T. 2012. Genetically encoded optical indicators for the analysis of neuronal circuits. *Nat Rev Neurosci* 13: 687-700
Kuhn B, Denk W, Bruno RM. 2008. In vivo two-photon voltage-sensitive dye imaging reveals top-down control of cortical layers 1 and 2 during wakefulness. *Proc Natl Acad Sci U S A* 105: 7588-93
Kuhn B, Fromherz P. 2003. Anellated hemicyanine dyes in a neuron membrane: Molecular Stark effect and optical voltage recording. *J Phys Chem B* 107: 7903-13
Kuhn B, Fromherz P, Denk W. 2004. High sensitivity of Stark-shift voltage-sensing dyes by one- or two-photon excitation near the red spectral edge. *Biophys J* 87: 631-39
Kuhn B, Roome CJ. 2019. Primer to Voltage Imaging With ANNINE Dyes and Two-Photon Microscopy. *Front Cell Neurosci* 13: 321
Larkum ME, Nevian T. 2008. Synaptic clustering by dendritic signalling mechanisms. *Curr Opin Neurobiol* 18: 321-31
London M, Häusser M. 2005. Dendritic computation. *Annual review of neuroscience* 28: 503-32
Margrie TW, Brecht M, Sakmann B. 2002. In vivo, low-resistance, whole-cell recordings from neurons in the anaesthetized and awake mammalian brain. *Pflugers Arch* 444: 491-8
Mittmann W, Koch U, Hausser M. 2005. Feed-forward inhibition shapes the spike output of cerebellar Purkinje cells. *J Physiol* 563: 369-78
Moore JJ, Ravassard PM, Ho D, Acharya L, Kees AL, et al. 2017. Dynamics of cortical dendritic membrane potential and spikes in freely behaving rats. *Science* 355
Nakai J, Ohkura M, Imoto K. 2001. A high signal-to-noise Ca^{2+} probe composed of a single green fluorescent protein. *Nat Biotechnol* 19: 137-41
Pages S, Cote D, De Koninck P. 2011. Optophysiological approach to resolve neuronal action potentials with high spatial and temporal resolution in cultured neurons. *Front Cell Neurosci* 5: 20
Petersen CCH. 2017. Whole-Cell Recording of Neuronal Membrane Potential during Behavior. *Neuron* 95: 1266-81
Röcker C, Heilemann A, Fromherz P. 1996. Time-resolved fluorescence of a hemicyanine dye: Dynamics of rotamerism and resolvation. *J Phys Chem* 100: 12172-77
Roome CJ, Kuhn B. 2014. Chronic cranial window with access port for repeated cellular manipulations, drug application, and electrophysiology. *Front Cell Neurosci* 8: 379
Roome CJ, Kuhn B. 2018. Simultaneous dendritic voltage and calcium imaging and somatic recording from Purkinje neurons in awake mice. *Nat Commun* 9: 3388
Roome CJ, Kuhn B. 2019. Voltage imaging with ANNINE dyes and two-photon microscopy. In *Multiphoton Microscopy*, ed. E Hartveit: Springer Nature (Neuromethods)
Roth A, Häusser M. 2001. Compartmental models of rat cerebellar Purkinje cells based on simultaneous somatic and dendritic patch-clamp recordings. *J Physiol* 535: 445-72
Scholl B, Wilson DE, Fitzpatrick D. 2017. Local Order within Global Disorder: Synaptic Architecture of Visual Space. *Neuron* 96: 1127-38 e4
Segev I, London M. 2000. Untangling dendrites with quantitative models. *Science* 290: 744-50
Senseman DM, Salzberg BM. 1980. Electrical activity in an exocrine gland: optical recording with a potentiometric dye. *Science* 208: 1269-71
Smith SL, Smith IT, Branco T, Häusser M. 2013. Dendritic spikes enhance stimulus selectivity in cortical neurons in vivo. *Nature* 503: 115-20
Stark J. 1914. Observations on the effect of the electrical field on spectral lines I Transverse effect. *Ann Phys-Berlin* 43: 965-82
Stuart G, Spruston N, Häusser M. 2016. *Dendrites*. Oxford ;: Oxford University Press. xxi, 714 pages pp.
Stuart GJ, Sakmann B. 1994. Active propagation of somatic action potentials into neocortical pyramidal cell dendrites. *Nature* 367: 69-72
Stuart GJ, Spruston N. 2015. Dendritic integration: 60 years of progress. *Nat Neurosci* 18: 1713-21

446 Svoboda K, Helmchen F, Denk W, Tank DW. 1999. Spread of dendritic excitation in layer 2/3 pyramidal
447 neurons in rat barrel cortex in vivo. *Nat Neurosci* 2: 65-73
448 Tasaki I, Watanabe A, Sandlin R, Carnay L. 1968. Changes in fluorescence, turbidity, and birefringence
449 associated with nerve excitation. *Proc Natl Acad Sci U S A* 61: 883-8
450 Wang SS-H, Denk W, Häusser M. 2000. Coincidence detection in single dendritic spines mediated by
451 calcium release. *Nat Neurosci* 3: 1266-73
452 Waters J, Larkum M, Sakmann B, Helmchen F. 2003. Supralinear Ca2+ influx into dendritic tufts of layer
453 2/3 neocortical pyramidal neurons in vitro and in vivo. *The Journal of neuroscience : the official*
454 *journal of the Society for Neuroscience* 23: 8558-67
455 Wilms CD, Häusser M. 2015. Reading out a spatiotemporal population code by imaging neighbouring
456 parallel fibre axons in vivo. *Nature communications* 6: 6464
457 Wilson DE, Whitney DE, Scholl B, Fitzpatrick D. 2016. Orientation selectivity and the functional clustering
458 of synaptic inputs in primary visual cortex. *Nat Neurosci* 19: 1003-9
459 Yang W, Yuste R. 2017. In vivo imaging of neural activity. *Nature methods* 14: 349-59
460 Yasuda R, Murakoshi H. 2011. The mechanisms underlying the spatial spreading of signaling activity. *Curr*
461 *Opin Neurobiol* 21: 313-21

462

463 **Figures**

464

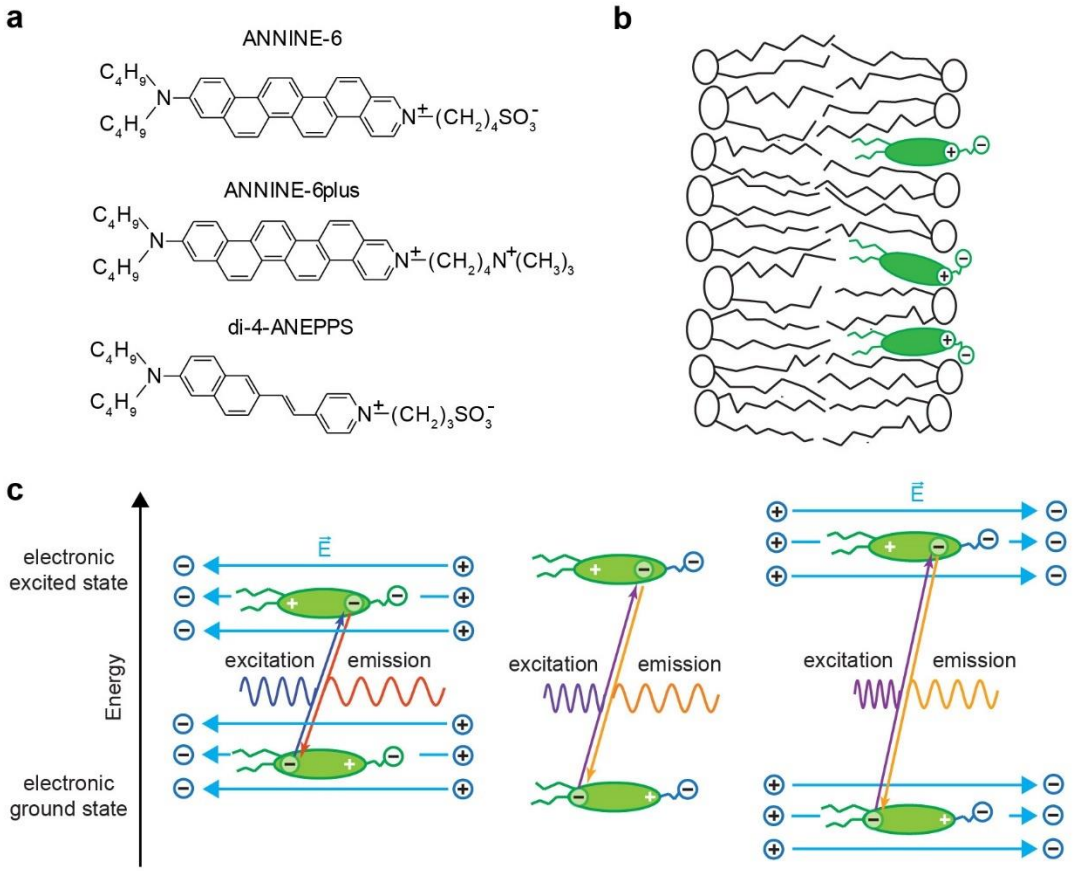

465

466 **Figure 1** Mechanism of voltage-sensitivity in electrochromic dyes. (a) Structure of three electrochromic
467 dyes, ANNINE-6, ANNINE-6plus, and Di-4-ANEPPS. (b) Due to their hydrophobic and hydrophilic
468 domains, electrochromic dyes bind to lipid membranes. (c) Excitation and emission of an electrochromic
469 dye molecule causes a charge shift within the chromophore (center). This charge shift is modulated by an
470 external electric field and shifts both the absorption and emission spectrum to either lower (left) or higher
471 energy (right), corresponding to higher and lower wavelength, respectively. (Kuhn & Roome 2019)

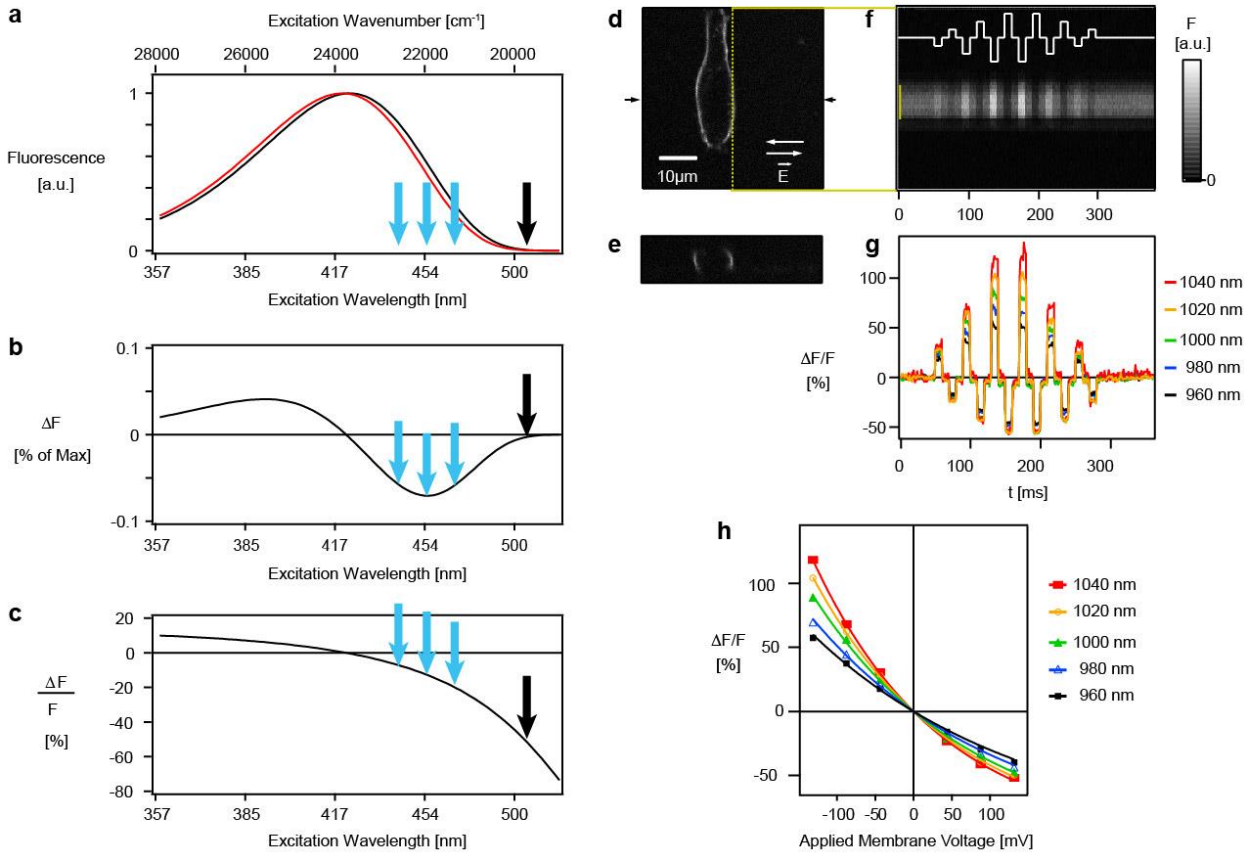

Figure 2 Optimizing voltage imaging with a charge-shift probe by excitation at the red spectral edge of absorption, exemplified by ANNINE-6. (a) An external electric field shifts the excitation and the emission spectrum. In this example, the absorption spectrum of ANNINE-6 in the outer lipid membrane leaflet of a neuronal membrane at resting potential (black) is shifted by a 100 mV membrane voltage change (red), corresponding to an action potential. The spectral shift is about 3 nm. (b) The difference between the two spectra, the fluorescence change ΔF, shows a maximum and a minimum at the steepest slope of the spectrum. (c) The fluorescence change normalized by the spectrum at rest results in the relative fluorescence change ΔF/F. The relative fluorescence change diverges at the red spectral edge of absorption. If a white light source – i.e. the photon output is distributed over a wide spectral range - is used for voltage imaging experiments, the signal ΔF is optimized by exciting a range around the steepest spectral slope (blue arrows, excitation band of about 440 to 470 nm). The ΔF integral of this spectral range is proportional to the detected voltage signal. With laser excitation, however, it is possible to optimize the relative fluorescence change ΔF/F or sensitivity by excitation at the red spectral edge of the absorption spectrum (black arrows). ΔF/F is a measure of information gained per detected photon, and it rises steeply at the spectral edge. As the absorption cross-section in this spectral range is very low, practically infinitely bright light sources with

narrow spectral range, such as lasers, are required for this optimization to reach a sufficient intensity level above photon shot-noise. Experimentally, the increase of sensitivity at the red spectral edge of absorption can be shown with one-photon excitation (Kuhn et al 2004) and, here, two-photon excitation at twice the excitation wavelength of one-photon excitation. (d,e) A HEK293 cell labeled with ANNINE-6 (f) is exposed to external electric fields (field direction indicated by arrows in (d)) while scanning along the membrane with two-photon excitation. (g) By increasing the excitation wavelength, the responses for the same membrane voltage change get larger. The excitation power of the laser is increased to keep the measured fluorescence intensity constant when exciting closer to red spectral edge of absorption. (h) The responses are linear in the physiological range of membrane voltage changes. Modified with permission from Elsevier (Kuhn et al 2004).

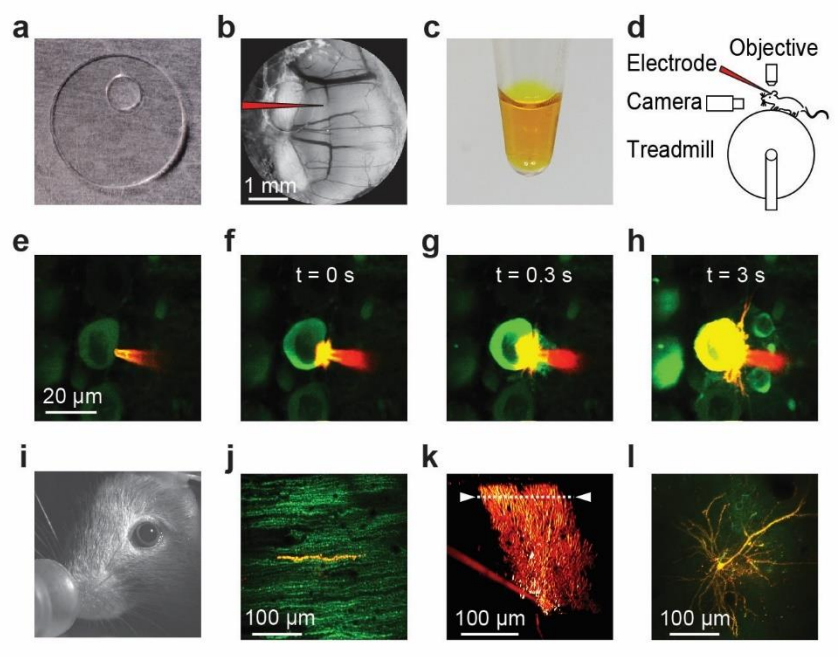

Figure 3 Double-labelling individual neurons for combined voltage and calcium two-photon imaging in awake mice. (a) 5-mm glass cover slip with silicone access port (Roome & Kuhn 2014). (b) A chronic cranial window with access port on the vermis of the cerebellum allows access to the brain with a pipette (schematically indicated). (c) ANNINE-6plus dissolved in pure ethanol at 3 mM concentration. (d) Sketch of the setup with a mouse mounted on a treadmill under a two-photon microscope. An electrode is used to fill single neurons by electroporation and to electrically record from their soma. A behavioral camera allows detailed observation of the pupil, the vibrissa, and the face of the mouse. (e-h) A patch pipette filled with ANNINE-6plus/ethanol solution is used to label single GCaMP6f expressing neurons by electroporation in the anesthetized mouse. (i) During the imaging experiment the mouse is fully awake, sitting on a treadmill and monitored with behavioral a camera. 24 hours after labelling a Purkinje neuron with ANNINE-6plus, the dye has spread out evenly, as can be seen in (j) the cross section of the Purkinje neuron dendrite as an overlay of the green channel (GCaMP6f) and the red channel (ANNINE-6plus) and in (k) the reconstruction of the Purkinje neuron in the red channel (ANNINE-6plus). The dotted line indicates the line scan position used in Fig. 4 and 5. It is also possible to fill other neurons with ANNINE-6plus by electroporation, as, for example, (l) cortical layer 2/3 pyramidal neurons shown as overlaid z-projection of the green channel (GCaMP6f) and the red channel (ANNINE-6plus). (Roome & Kuhn 2019)

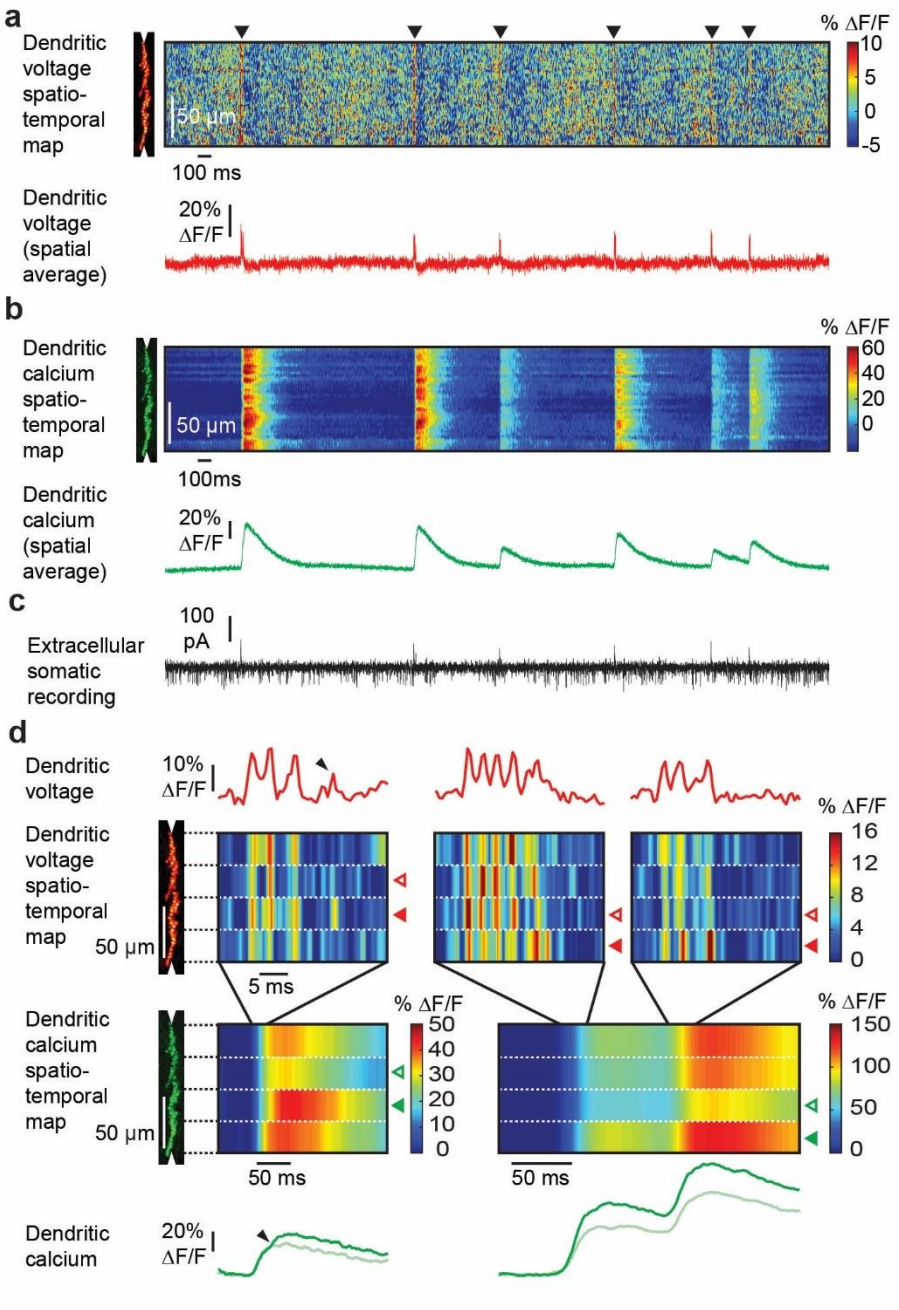

Figure 4 Simultaneous voltage and calcium imaging of Purkinje neuron dendrites and somatic recording in the awake mouse. (a) A line scan at 2 kHz was taken along the Purkinje neuron dendrites (scan position shown in Fig. 3j) to record a voltage spatio-temporal map in an awake mouse. The spatially averaged dendritic voltage (red trace) clearly shows suprathreshold dendritic complex spikes (black triangles). (b) The corresponding dendritic calcium spatio-temporal map and spatially averaged dendritic calcium (green trace) shows large calcium transients for every dendritic complex spike. (c) The access port also allowed simultaneous extracellular electrical recordings from the soma (black trace) while imaging voltage and

calcium transients from the dendrites. Simple spikes (somatic Na^+ spikes) result in a current sink at the soma, while complex spikes (dendritic Ca^{2+} spikes) result in a dominant current source signal at the soma. (d) Different parts of the dendritic tree show a different number of spikelets during the same complex spike event. The number of spikelets correlate with the amplitude of the calcium transients in each part of the dendritic tree. Open arrowheads indicate spatially localized low activity, filled arrowheads show high activity. Spatially localized dendritic spikelets during complex spikes correlate with a local boost in the dendritic calcium transient (small arrowheads). (Roome & Kuhn 2018)

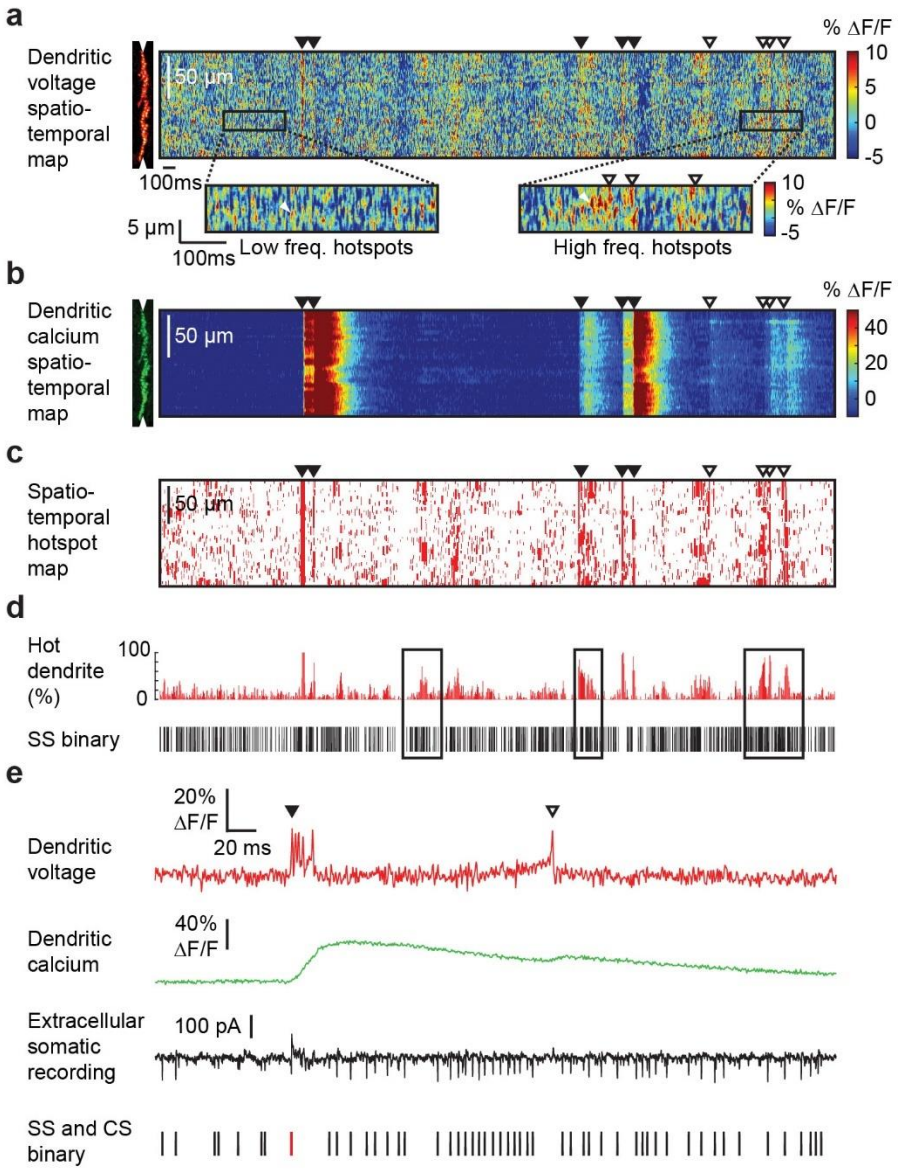

Figure 5 Sub- and suprathreshold dendritic signaling in awake mice. (**a**) Dendritic voltage spatio-temporal maps show epochs of low and high frequency subthreshold 'hotspot' events in Purkinje neuron dendrites (scan position shown in Fig. 3j). White arrow heads indicate single hotspot events. (**b**) The corresponding calcium spatio-temporal map does not show any correlated calcium transients except following suprathreshold complex spikes and dendritic spikes indicated in (a) by filled and open triangles, respectively. (**c**) By thresholding and additional spatio-temporal selection criteria, a spatio-temporal hotspot map can be generated. (**d**) Hotspot activity correlates with the simple spike (SS) activity at the soma. (**e**) Spatially averaged dendritic voltage (red) and calcium (green) recorded at 2kHz, reveal rapid (1-2 ms) and

variable suprathreshold dendritic spikelets during complex spikes (filled triangle). Extracellular somatic recordings (black) were used to identify the somatic output signals; simple spikes (SS: black binary trace) and complex spikes (CS: red binary trace). Non-climbing fiber evoked suprathreshold dendritic calcium spikes (open triangles) were detected in the awake mouse which enhance local calcium influx and showed no coincident sodium influx (simple spike) at the soma. (Roome & Kuhn 2018)